45 Years of Modelling Gas Explosions with the PDR Concept – Current Status and Future Prospects

Helene Hisken[1], Anand Zambare[2], Anish A. Pophale[2], Vagesh D. Narasimhamurthy[2], Kees van Wingerden[3], Trygve Skjold[1], Bjørn J. Arntzen[1,4], and Melodia Lucas[1,4]

[1] Department of Physics and Technology, University of Bergen, Allégaten 55, 5007 Bergen, Norway
helene.hisken@uib.no
[2] Department of Applied Mechanics & Biomedical Engineering, Indian Institute of Technology Madras, Chennai 600036, India
[3] Vysus Group, Kanalveien 7, 5068 Bergen, Norway
[4] Gexcon AS, Kanalveien 105, 5068 Bergen, Norway

Abstract. Accurate assessment of the consequences of explosions in systems where explosion hazards are present is necessary to ensure that the risk analyses for these systems give high-quality decision support. To represent explosions in systems of practical interest, consequence models must be able to account for the physical and chemical processes on the scales where the flame front and flow structures interact. Flame acceleration and overpressure generation in flammable fuel-air clouds are highly sensitive to the presence of geometry – parameters such as obstacle dimensions, orientation, shape, and distribution within the flammable cloud can significantly affect the severity of the event. Computational fluid dynamics (CFD) models that apply the porosity/distributed resistance (PDR) concept offer a pragmatic approach for modelling the effect of complex geometry on the highly transient and three-dimensional physical phenomena in gas explosions. The PDR concept was first adapted for modelling gas explosions by Bjørn H. Hjertager in the early 1980s, as part of his research activities at Chr. Michelsen Institute (CMI) in Bergen, Norway. Almost five decades later, several CFD models that apply the PDR concept for gas explosion simulations exist, both for academic and commercial use. The increase in computational capacity over the last decades allows for more widespread use of CFD simulations for risk assessments in industry and society. This paper reviews the recent advances in modelling gas explosion scenarios with the PDR concept, addressing challenges from a modelling perspective together with implications for the strength of knowledge in risk assessments. Furthermore, the paper discusses how academic study and practical application of these models can support the global energy transition.

Keywords: CFD, PDR, gas explosions, consequence modelling, risk analysis.

1 Introduction

Explosion hazards must be considered when planning, building, and operating systems that handle flammable gases and liquids [1, 2, 3]. To ensure that risk analysis for these

systems provides high-quality decision support, it is important that the consequences of gas explosion events are assessed with sufficient accuracy. Ideally, the uncertainty associated with these results should be documented and known to stakeholders. Pressure waves generated by explosions may produce projectiles, cause buildings to collapse, and lead to escalating events such as fires and releases of toxic or flammable materials [4]. Model results are normally required both to assess the consequences of selected 'worst case' or 'credible worst case' accident scenarios and for performing fully quantitative risk assessments (QRAs) that may entail simulating hundreds of scenarios and estimating the corresponding probabilities [5, 6]. A range of consequence models that predict the overpressure effects of accidental explosions have been developed over the last decades. These models are of varying complexity and applicability [7, 8].

A gas or vapour cloud explosion (VCE) event typically involves loss of containment of a flammable substance in an environment where geometry is present, providing confinement and congestion in the form of e.g. the ground, walls, tanks, pipes, water, cars, vegetation, etc. Releases of flammable gas will disperse and mix with the surrounding air (or other oxidiser), potentially creating a cloud through which a premixed combustion wave is able to propagate. The size and shape of the flammable cloud will depend on e.g. the release size and duration, ventilation, layout of the surrounding geometry, etc. Flammable liquids may evaporate to form a flammable mixture, provided the temperature exceeds their flash point. Alternatively, if a flammable liquid stored at a higher temperature is released, this may cause a flammable mist cloud. If the premixed fuel-air cloud becomes sufficiently reactive and finds an ignition source, a flame front can potentially accelerate through the cloud, generating damaging overpressures. The primary mechanism driving flame acceleration and overpressure generation in congested areas is the positive feedback between expansion of combustion products, generation of turbulence from obstructions in the unreacted mixture, and enhanced rate of turbulent combustion. Turbulence promotes combustion by increasing the mixing rate and heat transfer between combustion products and reactants, and by enhancing the surface area of the flame front [9, 10, 11]. The presence of obstacles with diameters as small as 1 mm may significantly increase flame acceleration in gas explosions [12, 13]. Various instability mechanisms will also promote flame acceleration [14].

To represent explosions in systems of practical interest, consequence models must be able to account for relevant processes on the scales where the flame front and flow structures interact. At the same time, for practical use in risk analyses, it may be necessary to assess explosion effects on scales up to several hundred meters. Effects of geometry (even on very small scales) are significant, and explosion consequences depend on scale, geometric configuration, and initial conditions in a non-linear fashion. Simulating gas explosions in realistic geometries therefore represents a complex multiscale modelling challenge.

In a review of consequence models by van Wingerden [8], four classes of explosion models for use in risk analysis are described: (i) far-field blast models, (ii) venting guidelines, (iii) phenomenological models, and (iv) dedicated computational fluid dynamics (CFD) models. CFD models solve the discretised Navier-Stokes equations for fluid flow, and can in principle account for the effect of varying boundary and initial

conditions, such as the size and complexity of the system, the degree of congestion and confinement of the geometry, varying levels of initial turbulence, concentration of the flammable cloud, etc. Hence, CFD models can be expected to represent a wide range of systems and scenarios, accounting for details and giving results with a higher level of accuracy for specific scenarios than the simpler models in classes (i)-(iii).

The increase in computational resources over the last decades has enabled widespread use of CFD in risk assessments. However, it is not possible to resolve all processes that lead to flame acceleration in large-scale systems with Direct Numerical Simulation (DNS). Models that use the Large Eddy Simulation (LES) approach can be applied for simple geometric configurations, but the simulations are computationally expensive and time-consuming. To test multiple scenarios and complicated geometries, applying LES models is currently impractical. Therefore, the most commonly used CFD models for predicting gas explosion consequences in risk assessments apply the Reynold-Averaged Navier-Stokes (RANS) equations together with a two-equation turbulence model. To represent the effect of complex geometry, these models use a common strategy: the *porosity/distributed resistance (PDR)* concept [15, 16].

The PDR approach was first proposed by Patankar and Spalding [17] to account for the effect of unresolved geometry on fluid flow in heat exchangers. Sha *et al.* [18] extended the concept to include advanced turbulence modelling. Hjertager [19] was the first to adopt the PDR concept for gas explosion modelling. The PDR concept captures two main effects of unresolved geometry on the simulated flow: (i) the total volume and area available to the flow are reduced, and (ii) geometry details introduce additional flow resistance and mixing. These effects are accounted for in the conservation equations for fluid flow as volume porosity (β_v) and area porosity (β_j). Here, β_j accounts for the area porosity in the jth direction. The porosities β_v and β_j are typically calculated for a specific geometry and computational grid in a preprocessing step, prior to solving the Navier-Stokes equations. A porosity calculator will read the information about the geometry (typically given in CAD format), and compute β_v as the ratio of open volume to the total volume of each grid cell, and β_j as the area available for flow in the jth direction. The porosities β_v and β_j will, for each grid cell, have a value between 0 (fully blocked) and 1.0 (fully open).

Finding the optimal algorithm for computing porosities for use in gas explosion modelling (e.g. accounting for numerous objects in a single grid cell, overlapping objects, aligning walls with grid lines, etc.) is not a trivial task. Furthermore, additional variables characterising the unresolved obstructions will normally be necessary for the modelling of sub-grid effects, such as the total wetted surface area of obstructions, characteristic dimension of obstructions, drag factors for different obstacle types, number of obstacles in the grid cell, etc. [20, 21, 22, 23].

This paper reviews the history and recent advances in the modelling of gas explosions with the PDR concept. Section 2 describes how the PDR concept was first introduced for explosion modelling in the 1980s and gives an overview of the developments over the last four decades. The presentation focuses on a few key aspects related to how the different models represent flame acceleration in turbulent flow past un-resolved geometry. Section 3 compares selected results from two different PDR models, to demonstrate how different model systems can both represent a hydrogen

explosion scenario. Section 4 discusses some of the modelling challenges in the context of recent model development and emerging applications. Finally, Section 5 summarises prospects for future development.

2 Model systems – history and recent developments

2.1 First application of the PDR concept for explosion modelling

Bjørn H. Hjertager initiated the development of FLACS around 1980 at Chr. Michelsen Institute (CMI) in Bergen, Norway [24]. Hjertager had previously been collaborating with Professor Bjørn F. Magnussen at NTH, the Norwegian Institute of Technology, conducting seminal studies on turbulent combustion modelling [25]. At CMI, research on dust explosions had already been established in the 1970s, led by Rolf K. Eckhoff. Due to these activities, in 1976, CMI was asked by Statoil (presently known as Equinor) to conduct a preliminary scientific assessment of the potential for gas and mist explosions at installations for oil and gas production [26]. This study provided the starting point for the extensive "Gas Safety Programmes" (GSP) at CMI in the 1980s. Hjertager led the first "Gas Safety Programme" from 1980-86, exploring the mechanisms of flame-turbulence interaction and flame acceleration in large-scale explosions. The first version of FLACS was released in 1986 [27]. Presently, the model is commercially available from Gexcon as "FLACS-CFD". In this paper, FLACS-CFD will be referred to as FLACS for brevity and historical reasons.

Hjertager [19] describes the underlying numerical model in FLACS, which is based on the Favre-averaged conservation equations for mass, momentum, and energy. In addition, equations are solved for the fuel mass fraction (Y_F) and the mixture fraction (ξ). For gas explosion simulations performed with FLACS, the mixture fraction denotes the degree of mixing between two pre-defined gas compositions – representing the premixed fuel-oxidiser component and the surrounding atmosphere, respectively. Turbulence effects are accounted for by applying the standard k-ε model [28], and conservation equations are solved for the kinetic energy of turbulence (k) and its rate of dissipation (ε). Accounting for the partial porosities, β_v and β_j, a generic equation for the variable Φ in the model can be expressed as

$$\frac{\partial}{\partial t}(\beta_v \rho \Phi) + \frac{\partial}{\partial x_j}\left(\beta_j \rho u_j \Phi\right) = \frac{\partial}{\partial x_j}\left(\beta_j \Gamma_\Phi \frac{\partial \Phi}{\partial x_j}\right) + \beta_v (S_\Phi + R_\Phi), \quad (1)$$

where ρ is the density, u_j is the velocity component in the jth direction, Γ_Φ is the effective turbulent diffusion coefficient, S_Φ is the source term for Φ, and R_Φ represents additional resistance, mixing, etc. caused by solid obstructions in the flow. The equations for k and ε read as

$$\frac{\partial}{\partial t}(\beta_v \rho k) + \frac{\partial}{\partial x_j}\left(\beta_j \rho u_j k\right) = \frac{\partial}{\partial x_j}\left(\beta_j \frac{\mu_{eff}}{\sigma_k}\frac{\partial k}{\partial x_j}\right) + G - \beta_v \rho \varepsilon, \quad (2)$$

$$\frac{\partial}{\partial t}(\beta_v \rho \varepsilon) + \frac{\partial}{\partial x_j}\left(\beta_j \rho u_j \varepsilon\right) = \frac{\partial}{\partial x_j}\left(\beta_j \frac{\mu_{eff}}{\sigma_\varepsilon}\frac{\partial \varepsilon}{\partial x_j}\right) + C_1 \frac{\varepsilon}{k} G - C_2 \beta_v \rho \frac{\varepsilon^2}{k}. \quad (3)$$

Here, μ_{eff} is the effective viscosity, σ_k and σ_ε are Schmidt/Prandtl numbers [24], and G is the production rate of turbulence. The k-ε model is extended with a production term for sub-grid turbulence production that depends on the partial porosities and properties of the sub-grid objects. The equations are discretised and solved on a structured Cartesian grid.

This general description of the model system from 1986 is still representative of the current version of FLACS-CFD (v24.2, released on January 15, 2025) [24]. However, the numerical schemes used to solve the equations, the strategy for combustion modelling, etc., have been further developed since the original release [21, 24].

One of the main challenges of modelling turbulent premixed combustion is to represent the Favre-averaged sink term accounting for consumption of fuel due to chemical reaction (R_{FU}) in the conservation equation for the Favre-averaged fuel mass fraction (Y_F). Due to the highly non-linear nature of R_{FU}, it is difficult to estimate this term using mean values. Instead, closure is normally obtained by physical analysis [29]. The combustion model implemented in the first versions of FLACS assumed that the rate of combustion is limited by the rate of molecular mixing between reactants in the flow, and hence that the combustion rate is proportional to the rate of dissipation of kinetic turbulence energy. Magnussen and Hjertager [25] argued that for fast chemistry, the reaction rate in the fuel mass fraction equation (R_{FU}) can be expressed in terms of a limiting mass fraction m_{lim}, where m_{lim} is the smallest of the mass fractions for fuel, oxygen or burnt products. Hence, $R_{FU} = -A\ \rho\ \varepsilon/k\ m_{lim}$, where A is a constant. Furthermore, Hjertager [19] presented a modified expression for the reaction rate to account for quenching, where the criterion for combustion relates to the ratio of a chemical timescale (τ_{ch}) to a timescale representing the lifetime of the turbulent eddies (τ_e). A model for representing the quasi-laminar phase of combustion in the initial phase of flame propagation, and the transition from laminar to turbulent combustion, was developed and implemented by Bakke and Hjertager (1986) [30, 31].

2.2 Model development after Piper Alpha (1988)

The development of models for predicting gas explosion effects was accelerated after the Piper Alpha disaster in 1988, which claimed 167 lives and "*led to new offshore safety regulations and standards that since have been accepted around the world*" [27]. Over the next two decades, several consequence models were developed in parallel with extensive experimental investigations [32]. The experimental work provided new knowledge about the physics of industrial-scale gas explosions, supporting both model validation and further development [7, 8, 33, 34, 35, 36]. In particular, four CFD models for gas explosion applications were further developed and tested as part of the CEC (Commission of the European Community) sponsored research programmes MERGE (Modelling and Experimental Research into Gas Explosions) and EMERGE (Extended MERGE) in the 1990s: FLACS, EXSIM, AutoReaGas and COBRA [34, 35]. COBRA was developed by British Gas Research and Development [37, 38, 39], and seems to have applied adaptive mesh refinement (AMR) to resolve the flame front and the flow around obstacles. The primary references in the open literature do not mention how the

PDR concept is used in the model. COBRA is therefore not discussed in further detail here.

EXSIM was developed by Hjertager at Tel-Tek, in cooperation with Shell, and is now commercially available from DNV [42, 44]. The CFD tool applies the PDR concept as described in the general equation (1), using the standard k-ε model to represent turbulence effects (cf. equations (2) and (3)). EXSIM is based on the same general modelling approach as FLACS. However, these two model systems were developed by separate groups in the 1990s, and have adopted different strategies for representing premixed combustion in gas explosions. In the following, the current modelling approach (as described in the open literature) for representing flame propagation past sub-grid obstructions in EXSIM is described first, followed by a brief review of how it relates to the modelling approach in FLACS.

The general expression for the resistance R_i from obstructions in the momentum equation in EXSIM is given as

$$R_i = -f_i A_w \frac{1}{2} \rho |u_i| u_i \ , \quad (4)$$

where A_w is the wetted surface area of obstructions per unit volume in the grid cell, and f_i is a function that varies depending on porosity, velocity, the distance between obstacles (pitch), typical dimension/hydraulic diameter, obstacle orientation, and shape. Different expressions are used for flow past a single obstacle in a control volume, and for flow through/parallel to rod bundles [20, 40, 41, 42]. Equation (4) relates to the additional source terms in equations (2) and (3) to account for the effect of un-resolved obstructions on turbulence production. The production rate of turbulence, G, is the sum of turbulence production from shear stresses in the fluid flow (from the resolved situation without partial porosities, G_s) and the turbulence production from sub-grid obstructions (G_R). The term G_R is expressed as

$$G_R = C_B |u_i| R_i \ ,$$

where R_i is the added resistance to the flow from sub-grid obstructions from equation (4), and C_B is a constant which has been calibrated to fit experimental data [41, 42].

After extensive validation against experiments in the 1990s, the contribution of G_R to the production term of ε in equation (3) was modified in EXSIM. The turbulence length scale in densely packed regions is imposed (i.e. set to a fraction of the characteristic dimension of the obstacles) rather than found by solving the conservation equation for ε [35, 41]. For turbulent combustion, EXSIM uses the eddy dissipation model with the quenching modification as suggested by Hjertager [19]. In addition, the reaction rate is enhanced by a factor E_t to account for flame acceleration when there are multiple obstacles present inside a grid cell [35, 41].

Similarly to EXSIM, FLACS applies the k-ε model with additional source terms for sub-grid contributions according to equations (2) and (3), and assumes that the production of turbulence due to sub-grid obstacles can be related to the added flow resistance (as expressed in equation (2)) [24, 34]. FLACS development in the 1990s resulted in several significant updates to the model system, and many of these are still used in the present version [24]. In his doctoral thesis from 1998, Arntzen [21] analysed the behaviour of the turbulence model and the combustion model in FLACS. Rather

than applying a mixing-controlled combustion model, he recommended computing the burning velocity by empirical correlations, and use this to define a reaction rate such that the numerical flame front would propagate with the designated velocity. The analysis that links the reaction rate to the burning velocity is based on deriving an eigenvalue of the 1D steady transport equation for the progress variable *c*. The progress variable can be related to the fuel mass fraction Y_F as $c=1-Y_F/Y_{F0}$, where Y_{F0} is the fuel mass fraction that was initially available in the specific computational cell, as presented by Catlin and Lindstedt [45].

This combustion modelling approach was also adopted by Catlin, Fairweather and Ibrahim in the COBRA code [37]. These authors emphasised that by using a mixing-controlled combustion model, a unique burning velocity will not be modelled unless a quench criterion is imposed on the solution, ensuring that the reaction rate falls to zero sufficiently rapidly as the cold front is approached. Without a quench criterion, the numerical flame front thickness and reaction rate will grow without bounds [45]. They also pointed out that a sufficiently fine resolution of the flame front is required to ensure a unique solution in transient computations, indicating that at least four cells must be used to resolve a representative length scale of turbulence.

Following the analysis by Arntzen [21], the numerical flame in FLACS was thickened by enhancing the diffusion rate and reducing the reaction rate in the flame zone through a so-called β-transformation. This was done to minimise the effect of numerical diffusion on the flame front. The thickened flame model is still used in FLACS, together with burning velocity correlations for the various regimes of flame propagation [24]. For the turbulent regime, the correlation by Bray [47] is used, where the turbulent burning velocity u_t is expressed in terms of the turbulence velocity u' and the Karlovitz stretch factor $K=0.157(u'/u_l)^2(u' l_I /u_l)$ (where u_l is the laminar burning velocity of the mixture and l_I is the integral length scale) as

$$u_t = 0.875\, u' K^{-0.392} . \qquad (5)$$

Arntzen [21] formulated an alternative burning velocity correlation specifically for low turbulence levels. For values of *K* exceeding 1, a quench criterion is applied to the turbulent burning velocity.

The analysis of Arntzen [21] resulted in an updated treatment of turbulence effects and flame surface area generation from sub-grid objects in FLACS. The sub-grid flame folding model directly enhances the burning velocity with a factor Ξ_s in the computational cell where there is an unresolved obstacle that gives a non-zero value of the parameter T_j. Here, $T_{j+} = \gamma\, a_{j+}/A_j$, where a_{j+} represents the area of the object's "end" inside the grid cell in the positive *j* direction, A_j is the area of the grid cell, and γ is a constant that depends on the shape of the object. Similarly, T_{j-} is defined for flow in the negative direction. These parameters are computed for every grid cell, in the positive and negative *x, y* and *z*-directions, and the contributions from separate objects are added together in each grid cell. The increase in flame surface area from unresolved obstructions is defined as

$$\Xi_s = 1 + \frac{\Delta A_F}{A_F} = 1 + C_{fl} \quad \overline{U_c}\, \varphi_j\, T_j ,$$

where ($\Delta A_F/A_F$) is the increase in flame surface area from the sub-grid obstacle, C_{fl} is a constant, U_c is the downstream flow velocity normalised by the speed of sound, and φ_i is a direction vector. The formulation assumes that the flame surface area increase from the flame front folding around an obstacle is proportional to the size of the obstacle and the ratio of the downstream flow velocity to the turbulent burning velocity (and assumes the turbulent burning velocity to be proportional to $U^{0.5}$). A higher flow velocity relative to the burning velocity means that the flame surface structures from the interaction with the obstacle is transported further downstream before the wake is fully burnt [21, 46].

The PDR model AutoReaGas was developed by TNO Prins Maurits Laboratory in the Netherlands [34, 66]. The gas explosion model was integrated with tools to also describe propagation of blast waves, blast loading, and structural response [7]. According to van den Berg *et al.* [65] and Salzano *et al.* [66], AutoReaGas mainly applied the same modelling approaches as EXSIM and the earlier versions of FLACS. In his review from 2013, van Wingerden [7] reported that the development of AutoReaGas was discontinued after 2005.

2.3 Model development after 2000 – extending the application domain

From 2000 onwards, there was significant focus on experimental work and model development related to hydrogen safety. Efforts were initiated in 2001 to improve the validity of FLACS for hydrogen applications. Specifically, the burning velocity model for hydrogen-air mixtures was updated to address Lewis number effects, and FLACS was subsequently validated for a wide range of hydrogen-related experiments [49]. Additionally, variables that allow the user to assess whether detonation-to-deflagration transition (DDT) is likely to occur in hydrogen explosion simulations were implemented [50].

In the period 2010–2020, new initiatives were undertaken to fundamentally update the model system in FLACS. This was motivated by the objective to improve model performance both for explosions in vented enclosures [46, 51] (including the effect of flame instabilities), and in large-scale, open areas with densely congested regions (typical of onshore process facilities or FPSOs) [46, 58]. The latter application was studied in a series of experimental campaigns after the Buncefield incident in 2005 [55, 56, 57]. Several experimental campaigns that investigated aspects such as necessary criteria for DDT and methods for explosion mitigation were conducted between 2010 and 2020 [32, 58, 59, 60]. Some of these campaigns supported efforts to implement updated turbulence and combustion models in FLACS, including alternative two-equation turbulence models, turbulence length scale limiters, a combustion length scale based on geometric dimensions of sub-grid geometry, updated burning velocity correlations, and a transport equation for flame surface area due to sub-grid obstructions [46, 58, 64].

However, introducing significant changes to the modelling approaches is challenging for a tool that needs to retain acceptable performance for a wide range of scenarios and applications. At this point, FLACS had become the de-facto industry standard for assessing explosion loads in the offshore sector – a change in FLACS results effectively means that the risk picture for the industry also changes. Hence, it is

essential to document that model development overall leads to better representation of physics across the application range. The doctoral thesis by Both [61] explored whether optimisation of sub-grid model parameters by using neural networks to emulate model response would be a viable method for ensuring optimal model performance for FLACS over the tool's validated application range. Some form of parameter optimisation is normally necessary to ensure acceptable model performance in practice [22, 34, 41]. This is not surprising when considering the uncertainties associated with combining a range of empirical or analytical sub-grid models together in a complex model system, where most of the dominating physical phenomena are inherently under-resolved [46, 61]. Some common modelling challenges for PDR models are discussed further in Section 4.

The representation of sub-grid geometry and calculation of necessary parameters in FLACS have been continuously developed and improved in the commercial releases of the model, although the underlying modelling principles for the physical phenomena in gas explosions has remained similar since the 1990s. The software has been gradually developed to enhance robustness and ease of use [24].

Limited information is available in the open literature about the development of EXSIM in the 2000s and 2010s. However, in 2023, DNV presented improvements to the modelling of hydrogen explosions in EXSIM [44].

2.4 Recent PDR models for predicting gas explosion effects

In 2014, Puttock *et al.* presented initial results from a new model system for simulating gas explosions [22], where the ambition was to combine the PDR concept for gas explosion modelling with up-to-date solution techniques and a wide community of contributors on the open-source platform OpenFOAM. PDRFoam applies the PDR concept with the XiFoam model for turbulent combustion [68]. The XiFoam model calculates the variable Ξ, which for every control volume is the ratio of the average flame area per unit volume to the average flame area projected onto the mean direction of propagation per unit volume. At equilibrium, this can be interpreted as the ratio of turbulent burning velocity to the laminar burning velocity. The transport equation of flame surface area due to turbulence, Ξ_t, can be written as

$$\frac{\partial}{\partial t}(\beta_v \rho \Xi_t) + \frac{\partial}{\partial x_j}\left(\beta_j \rho u_j \Xi_t\right) = \varphi_\Xi |\nabla \Xi_t| + \beta_v \rho G \Xi_t - \beta_v \rho R(\Xi_t - 1)\,,$$

where φ_Ξ is the flux for Ξ_t, and $G\Xi_t$ and $R(\Xi_t - 1)$ are the generation and removal rates of Ξ_t, respectively. Flame wrinkling due to instability effects in the initial phase of flame propagation is also accounted for by Ξ_t, and the equilibrium expression for Ξ_t at high turbulence levels is given by the Markstein number dependent turbulent burning velocity correlation proposed by Bradley *et al.* [70]. Further details on the formulation of these terms are presented by Puttock *et al.* [68].

In PDRFoam, a pre-processor computes the necessary fields to characterise the geometry: volume and area porosities (β_v and β_i), wetted surface area (A_w), various area blockage parameters, characteristic obstacle parameters C_T and C_R, parameters accounting for the number of obstacles in a cell, and the representative obstacle

diameter (L_{obs}) on a Cartesian grid. As discussed earlier for EXSIM and FLACS, the effect of sub-grid obstructions in the momentum equation is represented as an additional drag term, R_i, with drag factors C_R that depend on obstacle shape, Reynolds number, and turbulence intensity [72]. The production term in the *k*-equation due to sub-grid obstacles, G_R, is on the same general form as proposed by Sha and Launder [46],

$$G_R = \frac{1}{2}\,\rho|u|(u \bullet C_T \bullet u) + C_{sk}\beta_v \mu_{eff} A_w^2\,(|u - u_s|)^2\,, \qquad (6)$$

where C_{sk} is a constant, the slip velocity u_s is zero, and C_T is a turbulence factor which is proportional to the drag factor [68, 69]. PDRFoam also includes a model for representing the sub-grid flame acceleration effect, enhancing the production rate of kinetic energy from sub-grid geometry as the flame propagates over several rows of obstacles.

Puttock *et al.* [22] list several convenient aspects of using the XiFoam model to simulate gas explosions. For example, the reaction rate is independent of flame thickness, and it is straightforward to add contributions to Ξ that represent different phenomena. The developers of PDRFoam have added the flame surface area due to sub-grid obstructions as a separate flame wrinkling factor, Ξ_s, to separate it from flame wrinkling due to turbulence, Ξ_t. The resulting turbulent burning velocity can then be estimated as

$$u_t = \Xi_t \Xi_s u_l\,.$$

This approach allows for the transport of flame surface area with the flow, which is not represented by the other PDR models. Puttock *et al.* [22] propose that flame surface area may increase over a short distance after exiting from a congested region, due to jetting of the flame between the obstacles, and argue that the combustion model in PDRFoam can be used to represent this effect. The transport equation for flame surface area due to sub-grid obstructions, Ξ_s, is on the same form as for Ξ_t, with an equilibrium value defined as

$$\Xi_{s,eq\Theta} = 1 + min\left[C_1 \overline{b_l}\,,\ \frac{C_2\,|u|}{u'} \overline{b_l}, C_3\right]^{N},$$

where C_1, C_2 and C_3 are constants, $|u|$ is the magnitude of the flow velocity, b_l is the area blockage in the direction of flame propagation, and N is the number of obstacles in a computational cell. The equilibrium expression for flame surface area increase due to sub-grid obstructions is based on observations from CFD simulations as presented by Puttock *et al.* [69]. A separate transport equation is solved to track the length scale of the flame wrinkling due to sub-grid obstructions [68].

Dhiman *et al.* [71] studied how the PDRFoam solver represents mean velocities and turbulence fluctuations in steady-state, two-dimensional, non-reacting flows past circular cylinders of diameter D, where the grid resolution Δy was varied between 2D and 0.06D. The authors compared the simulation results from PDRFoam with results obtained by using simpleFOAM (i.e. with resolved geometry) and experimental results from the EMERGE project [21]. They observed that for sufficiently fine resolutions,

the PDR solver reproduced the mean velocities and velocity fluctuations. However, when the grid resolution approached the cylinder diameter, velocities and velocity fluctuations were under-predicted, especially at distances several obstacle diameters downstream of the obstacle. Additional validation of the PDRFoam solver against explosion experiments was done by Dhiman *et al.* in 2023 [72]. This study focused on flame propagation past various configurations of pipes inside vented enclosures and partially confined geometries, using mixtures of methane and propane with air. Zambare *et al.* [73] used PDRFoam to simulate a series of hydrogen explosions in vented enclosures. Selected scenarios from this study are presented in Section 3.

The final PDR solver for gas explosion applications discussed here is STOKES (*Shock Towards Kinetic Explosion Simulator*), an in-house solver from the University of Campinas (UNICAMP), Brazil. Vianna and Cant [74] implemented the PDR concept into the NEWT solver, updating the approach for solving the Navier-Stokes equations on an unstructured grid. Vianna *et al.* [23, 75, 76, 77, 78] later implemented the PDR concept into STOKES. The porosities in STOKES are calculated using a Gilbert-Johnson-Keerthi (GJK) distance algorithm, which checks for collisions between an element of the mesh and each solid of the geometry [23, 75]. The model solves the conservation equations for mass, momentum, energy, the progress variable and the mixture fraction, and uses the standard k-ε model to account for turbulence effects. The representation of sub-grid geometry in the governing equations is similar to that presented for the other PDR models. The resistance term in the momentum equation is modelled as equation (4), with the same f_i as given for EXSIM in [20], and the production of turbulence from sub-grid geometry is the approach suggested by Sha and Launder [46], i.e. on the same form as equation (6).

In STOKES, the Bray-Moss-Libby (BML) combustion model is used to represent the averaged source term in the equation for the progress variable. The BML model assumes a probability density function for the progress variable, c. The reaction rate in the progress variable equation is estimated as $\rho_R u_l I_0 \Sigma$, where ρ_R is the density of the reactants, u_l is the laminar burning velocity, I_0 is a factor that accounts for flame extinction and stretch effects, and Σ is the flame surface area to volume ratio [77]. The integral length of wrinkling due to turbulence, L_y, controls the flame surface area Σ (see the discussion by Quaresma *et al.* [77] for further details). Empirical correlations are often used to model L_y. Quaresma *et al.* [77] suggested using a hybrid BML-fractal approach to model the reaction rate, where L_y is calculated by a fractal-based approach, while Quaresma *et al.* [78] presented a version of the BML model with a dynamic representation of the stretch factor I_0. The authors used STOKES to simulate both detailed experimental work as well as hypothetical gas explosions in large-scale chemical process modules.

Table 1 summarises the different approaches to combustion modelling in the model systems FLACS, EXSIM, PDRFoam, and STOKES. The history and present status of the model systems as presented in this section can be used to identify common modelling challenges and opportunities. Section 4 elaborates on these aspects.

Table 1. Overview of modelling approaches.

Model system	Turbulent combustion model	Sub-grid flame folding	Current use/status
FLACS	β-model with empirical correlations	Localised enhancement factor, depending on area blockage, obstacle type and flow speed.	Commercially available software.
EXSIM	Mixing-controlled (EDC)	Reaction rate enhanced by a factor E_t to account for several obstacles in a cell.	Commercially available software.
PDRFoam	Weller model	Separate transport equation for flame surface area due to sub-grid obstructions.	Open-source software.
STOKES	Bray-Moss-Libby	Not documented in the open literature.	In-house, academic solver.

3 Case study – vented hydrogen deflagrations

This section presents selected results from FLACS and PDRFoam for two explosion experiments from the HySEA project. The experimental campaign in HySEA comprised of 66 tests with vented deflagrations, performed in 20-foot ISO containers [79]. This configuration is directly relevant for real applications, such as hydrogen refuelling stations. For the present discussion, the objective is to demonstrate how two different PDR models represent the same experiment, considering the different sub-grid modelling approaches in the model systems. Detailed analysis of the experiments can be found elsewhere [63, 64, 79, 80].

The first phase of the experimental campaign in HySEA explored the effect of varying the type and level of congestion, vent panel configuration, ignition position, and concentration of homogenous hydrogen-air clouds inside the containers. Zambare *et al.* [73] simulated the first 14 tests of the campaign with PDRFoam, where the explosions were vented through one of the end walls. Results for tests 13 and 14 of the HySEA campaign are presented here. These tests involved a fuel-lean mixture of 21 vol% hydrogen in air, and the mixture was ignited at the back wall of the container (opposite to the vent opening). The doors of the container were fully open during the test, and the opening was covered by a plastic sheet to contain the flammable mixture prior to ignition. The obstacle arrays that were placed inside the container consisted of a pipe-rack and a bundle of gas bottles. The test configurations are illustrated in Fig. 1, denoted P1 and P1B3 for tests 13 and 14, respectively.

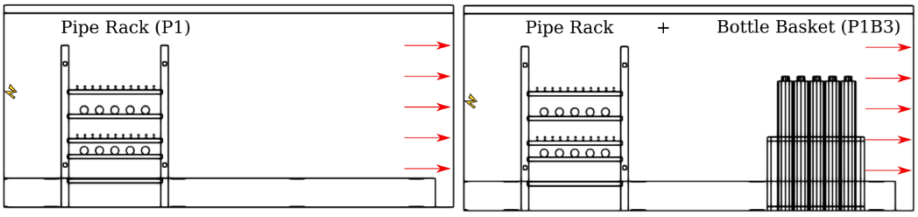

Fig. 1. Obstacle configuration for test 13 (P1, left) and test 14 (P1B3, right). Illustration from Zambare *et al.* [73].

The grid resolutions that were applied in the simulations with both model systems were determined based on previous validation against experiments [63, 73, 80]. For FLACS, existing guidelines were followed [24]. The FLACS simulations applied a grid resolution of 0.15 m in the core domain (i.e. in the region where most of the combustion occurs). PDRFoam used a grid resolution of 0.24 m (cf. the discussion by Zambare *et al.* in [73]). The FLACS results presented here have been obtained using an in-house development version of the tool, using an alternative combustion model that explicitly depends on the Markstein number of the mixture. This combustion model is described in further detail by Lucas *et al.* [64].

The explosion overpressure was recorded in eight positions throughout the container, close to the walls, and at three locations outside the container opening. Fig. 2 shows experimental and simulated pressure-time histories from one of these locations inside the container, from tests 13 and 14 (with obstacle configurations P1 and P1B3, respectively). In Fig. 2, the experimental pressure-time histories have been post-processed with a Savitzky-Golay filter [81], filtering out frequencies exceeding 50 Hz. The figure also marks the simulated time of flame arrival at the first obstacle (green vertical lines), and the simulated time of flame exit from the enclosure (red vertical lines).

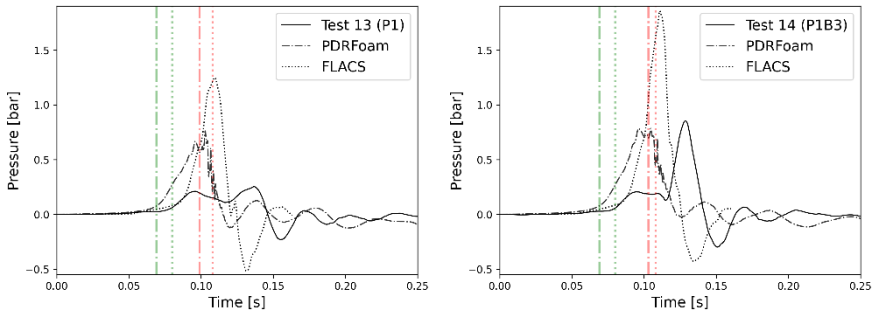

Fig. 2. Pressure-time curves from tests 13 (left) and 14 (right), from inside the container. Green vertical lines denote the simulated arrival of the flame front at the pipe rack, while the red vertical lines denote the arrival of the simulated flame front at the vent opening (dotted vertical lines are for FLACS, dash-dotted vertical lines are for PDRFoam).

Unfortunately, flame speeds could not be recorded in the experiments, as there was no visual access inside the containers. However, flame arrival along the centre line of the

container can be analysed in the simulations. Fig. 3 shows the flame position vs. time for tests 13 and 14, predicted by both FLACS and PDRFoam.

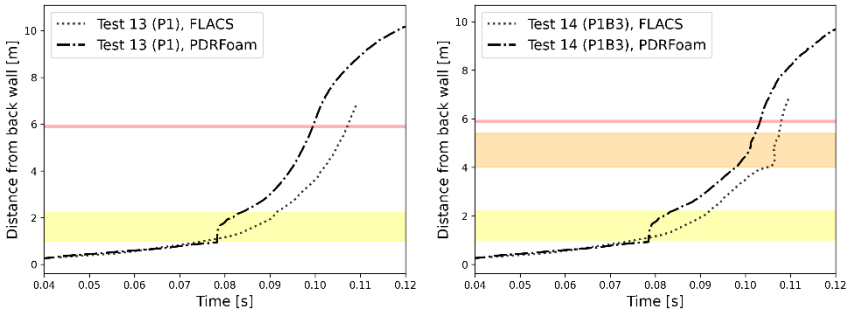

Fig. 3. Simulated flame arrival at distance from back wall vs. time, measured along the centreline of the container for test 13 (left) and test 14 (right). The yellow and orange horizontal areas mark the position of the P1 and B3 obstructions inside the container, respectively. The horizontal red line marks the position of the vent opening.

The development version of FLACS gives conservative predictions of the explosion pressure in the container for both tests. In both scenarios, the maximum pressure occurs as the flame front reaches the vent opening. The bottle rack (B3) is dense and acts more like a single, large obstacle on the flow than the more sparsely packed pipe rack (P1). The bottles are blocking the outflow through the vent opening and thus reducing the pressure relief during the explosion in test 14 with obstacle configuration P1B3. The flame first decelerates as it approaches B3, before it is pushed above and around the bottle rack before propagating completely through the narrow spaces around the bottles. Hence, there is uncertainty associated with the predicted flame position through B3 as plotted in Fig. 3 (right). The predicted overpressure from PDRFoam appears to be relatively insensitive to the change in congestion from test 13 (P1) to test 14 (P1B3). From Fig. 3, the most significant flame acceleration in PDRFoam seems to occur as the flame front passes through P1.

Fig. 4 visualises the combustion products from FLACS (left) and PDRFoam (right), as the simulated flame front is approaching B3 in test 14. Fig. 5 shows the reaction rate (top) and the turbulent burning velocity (bottom) from PDRFoam at the same instance in time as in Fig. 4 (right). This time corresponds to the occurrence of the maximum overpressure in the PDRFoam simulations. At this moment, the highest combustion rates as predicted by PDRFoam occur at the P1 piperack. In Fig. 6, the reaction rate and turbulent burning velocity in FLACS is plotted at the time of maximum overpressure for test 14. This event occurs just prior to the exit of the flame front from the vent opening, as the flame propagates through the bottle rack (B3).

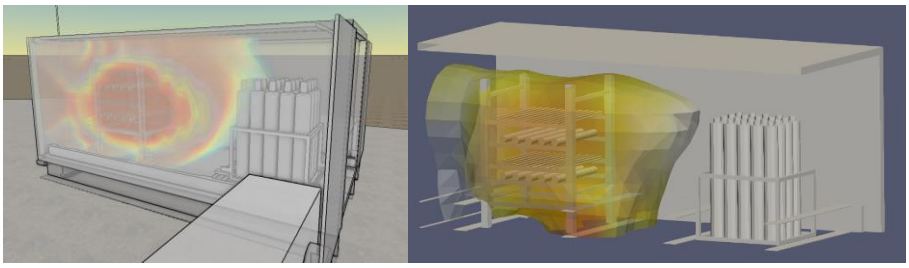

Fig. 4. Simulated combustion products in FLACS (left) and PDRFoam (right).

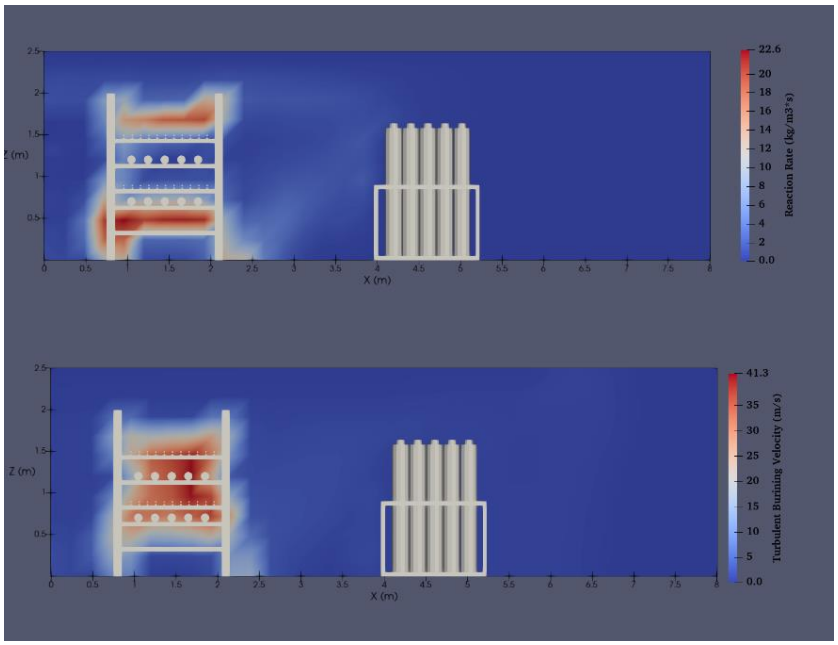

Fig. 5. Reaction rate (top) and turbulent burning velocity (bottom) from PDRFoam.

Since the information about the explosion mechanism from these two experiments is limited, it is challenging to further analyse the model results in terms of agreement with experimental results. Additional experiments should be studied to further explore the different modelling approaches in FLACS and PDRFoam. Moreover, this discussion does not consider the general capabilities of the model systems in terms of validation and user friendliness. The HySEA experiments have been simulated in several previous studies that provide more detailed analysis than what is covered here [63, 64, 80].

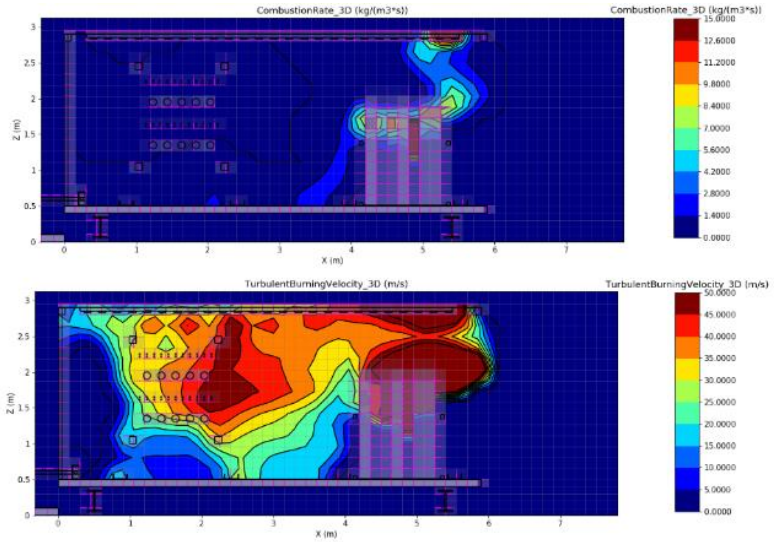

Fig. 6 Combustion rate (top) and turbulent burning velocity (bottom) in FLACS for test 14, at the time of maximum overpressure.

4 Modelling challenges

Balancing model complexity and computational efficiency is one of the most important features of PDR models. It is interesting to note the overall similarity between the CFD solvers presented in the previous sections, and yet how different solutions have been applied to address the main modelling challenge: representing premixed turbulent combustion in a propagating flame front in large-scale, complex systems, where the dominant physical phenomena are un-resolved, transient and highly sensitive to small-scale effects.

Significant dependency of results on grid resolution and retaining valid results as the relative resolution of various processes varies (both as the explosion progresses and between scenarios), seems to be common challenges for PDR models [42, 46, 73]. The transition between on-grid and sub-grid representation of geometry, and its effect on flame acceleration in gas explosions, is particularly challenging to represent [22]. Several studies have investigated the mean velocity, turbulence velocity, and length scales downstream of objects for a range of different grid resolutions to explore how the *k*-ε turbulence model with the PDR concept handles this transition [21, 34, 68, 71]. Most of the available results are for steady-state, non-reactive flows, for which experimental results exist. Results from resolved simulations are sometimes used to complement the available experimental data [68, 71].

Narasimhamurthy *et al.* [16] explain why there is limited data from experiments on turbulence generation in gas explosions. Following ignition, the flow speed in gas explosions typically accelerates from near-quiescent conditions to sonic or supersonic speeds, before going back to quiescent conditions in less than a few seconds. Therefore, each explosion test produces only a single transient signal in each location. Since

performing ensemble averaging over hundreds or thousands of repeated tests would be required to separate turbulent fluctuations from the transient mean-momentum, reliable measurements of turbulence in large-scale systems becomes prohibitively expensive. One of the few attempts at generating relevant data sets on turbulence measurements in transient flow similar to that in gas explosions were conducted by Kong and Sand as part of the Gas Safety Programmes and the EMERGE project in the 1990s [82, 83].

Arntzen analysed the limitations of the k-ε model for modelling gas explosions in FLACS in his doctoral thesis [21], focusing specifically on the effect of transient, reactive flow with or without sub-grid geometry. He noted that sufficient resolution of the mixing length scale in the flow was necessary to ensure rapid buildup of turbulence without the use of modified sub-grid models for *resolved* geometries. Meanwhile, the transient build-up of turbulence from *sub-grid obstructions* was found to be appropriate for gas explosion simulations. Furthermore, Arntzen observed that the turbulence length scale and dissipation downstream of sub-grid objects were highly grid dependent, and therefore not suited as input to a turbulent burning velocity model. To produce representative fields for the turbulence length scale/dissipation, he suggested that the sub-grid production of turbulence dissipation should be independent of the turbulence field. Finally, Arntzen emphasised the well-known issue with using the k-ε models in flows with high dilatation (e.g. flows with premixed combustion), which will lead to the production of unphysical turbulence in the flame zone, if the turbulence model is not adjusted to account for this [21]. The numerically thickened flame in FLACS-CFD implies that there also will be a transition between on-grid and sub-grid flame folding that must be handled by the combustion model.

In his doctoral studies, Sæter [39] studied the grid dependency of non-reactive flow in both steady and transient flow through 1D representations of obstructed regions in EXSIM. Consistently with the findings of Arntzen [21], he found that the turbulence length scale was particularly grid dependent. In transient flow, the build-up of the turbulence length scale was slower than for the other turbulence variables. In EXSIM, the dissipation of turbulence generated by sub-grid objects was modified to fit experimental data, leading to higher values of ε/k and hence higher combustion rates just downstream of bluff bodies. Sæter [39] found that this to some extent reduced the grid dependency of the solver. In PDRFoam, the dissipation associated with sub-grid obstructions is also treated separately from that of the "on-grid" turbulence [68]. The present version of FLACS [24] does not use the turbulence length scale as derived from the k-ε model in the turbulent burning velocity correlation. Instead, models based on the geometric characteristics of the system have been formulated [46, 63].

In gas explosions, a combustion model and a numerical flame front is introduced to the turbulent flow field, and it is not trivial to separate the effect of small-scale turbulence, instabilities and large-scale flame folding on the observed flame speed and explosion overpressure. When a combustion model that is highly sensitive to modelled turbulence variables determines the rate of flame acceleration in a complex model system, minor inaccuracies in the separate modelling approaches can be significantly enhanced. In practice, the turbulence model (specifically the sub-model representing the effect of unresolved geometry) will be modified and optimised together with other sub-grid models to fit results from selected gas explosion experiments. Evaluating

model performance by measuring how the model represents lumped effects can mask out shortcomings of the separate sub-models. This may become evident only when the model is used for a new application. An example is the application of PDR models for explosions in enclosures with vent openings and pressure relief panels. Although strictly not a "new" application, in vented explosions, mechanisms of overpressure generation other than flame acceleration through regions of sub-grid obstructions may dominate (such as flame instabilities and turbulence generated from flow past resolved objects and vent openings) [52, 53, 54]. These scenarios are challenging to represent, as the grid resolution in PDR models normally will not be sufficient to fully capture the driving mechanisms, and the sub-grid models may not have been developed or tuned to represent the necessary physical phenomena.

However, in a short-term perspective, it is not feasible to fundamentally solve each separate modelling issue for representing gas explosions in large-scale, realistic systems. For engineering tools to be useful, they need to both be readily available and give results that are sufficiently accurate for the purpose.

Developing user guidelines that are based on validation against experiments enables the use of CFD tools for risk analysis [24, 73]. Such well-documented guidelines are formulated to ensure that new scenarios (for which experimental results are unavailable) can be simulated with an expected level of accuracy, provided that the same physical phenomena as in the experiments are involved. Using validation results as a basis, methods for automatically defining appropriate simulation setups can be developed and integrated with the consequence model. For example, methods for automatic gridding are available in both FLACS and EXSIM [24, 42]. Another solution for addressing the specific problem with grid dependency is to implement adaptive mesh refinement (AMR) and, for example, ensure sufficient resolution over the flame front gradient for the modelling approach. However, it is not straightforward to integrate AMR with the PDR concept, and this functionality is not yet fully integrated in the model systems presented here.

The complex physical phenomena in gas explosions, along with the requirements for consequence models to represent a wide range of scenarios, is challenging for model development. It may not be straightforward to modify a part of the model system to better represent a phenomenon without compromising accuracy for other applications. Indeed, a parameter optimisation study performed for FLACS [61] showed that results were sensitive to many of the same parameters across validation cases, and relatively few model parameters were considered suitable for optimisation. This limits the potential for improving model results without introducing additional sub-grid models, but makes the model system easier to understand and manage. The model system in PDRFoam applies a more complex approach to modelling flame propagation in gas explosions than the equilibrium expressions in e.g. FLACS [46, 68]. PDRFoam solves separate transport equations for flame wrinkling due to turbulence, sub-grid obstacles and the length scale of sub-grid obstacles, and Puttock *et al.* [68] use around 23 combustion model constants. This approach allows for representing more complex phenomena (such as the increase in flame surface area after the flame front exits a congested region), but it is more challenging to assess the effect and the optimal value

of each constant in different situations. Optimal parameters may also change with varying resolution in space and time.

Relying on experimental data for model validation highlights another modelling challenge, i.e. the limited access to high-quality experimental data that is relevant for real systems. Model development still relies on experimental data produced as part of the research campaigns in the 1990s [68, 74]. Although several large-scale campaigns have been conducted since [32], the significant costs associated with these campaigns imply that there is limited possibility of repeating experiments (and thereby explore variability in phenomena as well as uncertainty associated with initial/boundary conditions and measurement errors). Furthermore, detailed results are not necessarily made available to the general research community. This effectively limits the possibility of stakeholders who have not been involved in the consortia to develop and improve their consequence models. It also limits the ability of users of consequence models to perform independent validation and explore model sensitivity. Validation reports and summaries are typically provided by commercial model developers, but these often provide limited information and therefore require the user to trust the developer. Blind-prediction benchmark studies show that lack of user experience with validation of cases that resemble the system under consideration can contribute to significant sources of error in model results [85]. It is therefore crucial that the developer provides the user with clear and unambiguous guidelines.

Sensitivity of model results to inaccuracies in the representation of certain physical phenomena may also be more pronounced as the reactivity of the mixture increases. This has implications for the increased use of PDR models for representing accident scenarios involving hydrogen mixtures, which are significantly more reactive and more prone to undergo DDT than mixtures with the traditional hydrocarbon-based energy carriers. Fuel-lean hydrogen-air mixtures experience enhanced combustion rates due to thermal-diffusive instabilities, caused by the imbalance between the mass diffusivity and thermal diffusivity of the mixture. Studies indicate that this effect is pronounced also in highly turbulent flames [70, 86], and should be represented by explosion models [46, 63].

Using CFD models to e.g. define safety distances, perform hazardous area classification, and determine the need for mitigation measures when designing hydrogen facilities is an attractive option, as risk owners and regulatory authorities navigate the lack of established standardised solutions and general knowledge about hydrogen systems and their hazards. Continued experimental work, model development and validation specifically for hydrogen applications is therefore crucial [63, 85].

5 Final remarks and future prospects

Bjørn H. Hjertager initiated the use of the PDR concept for gas explosion modelling in 1980. Half a century later, commercial CFD tools that apply the PDR concept still constitute the state-of-the-art for assessing explosion loads in systems where geometry effects cannot be neglected, such as in the offshore industry. Furthermore, the PDR

concept is also successfully used for simulating scenarios involving dispersion of flammable or toxic materials, jet and pool fires [24, 88].

Since the 1980s, the graphical interfaces and utility tools associated with the commercial models discussed here have been significantly improved to optimise user-friendliness. The integration of automatic methods for setting up and running simulations will likely only increase in the coming years. This implies that the user does not need to be an expert in CFD or explosion physics to get results that are supported by previous validation work, as well as ensuring that the model will be used within its range of applicability. Methods for surrogate modelling will likely also be used more widely, both by developers and final users. If successful, such methods allow exploring model sensitivity to variations in initial and boundary conditions, without the significant time requirements for running CFD simulations. The prerequisite for these developments is that the sub-models representing physical phenomena are sufficiently robust and general, and that validation has been performed against a sufficiently wide range of high-quality experiments. Hence, knowledge about physical phenomena and experimental data for gas explosions needs to be developed in parallel with these methods, to keep the uncertainty associated with the results on an acceptable level.

Validated CFD models that apply the PDR concept can both support and potentially accelerate the energy transition, as the three-dimensional, transient results from these models facilitate effective communication of risk. Results from PDR models can therefore contribute to building trust between the different stakeholders. As the transition towards more diverse use of energy carriers in society progresses, and the public are exposed to new, complex systems containing hazardous materials, the necessary knowledge about potential explosion hazards must be developed in parallel. However, the increased use of batteries and storage of hydrogen under temperatures and pressures that differ significantly from atmospheric conditions, as well as use of various blends of different fuels with hydrogen, inert gases and suppressants, requires consequence models that are able to represent a wider range of chemical processes on various timescales than the present PDR models currently are capable of [64]. This means that strategic experimental campaigns should be performed to fill the knowledge gaps, and that the data preferably should be made available to the relevant stakeholders – risk owners, authorities, risk analysts, researchers, software developers, etc., to enable more people to assess the risk associated with their systems and critically evaluate results from risk analyses. Experimental findings can be extended with results from models that resolve the geometry, the flame front and the largest flow structures. Models that apply LES together with detailed chemistry can potentially support the development of sub-grid models in PDR tools, for example by enabling the analysis of separate effects (flame acceleration due to increased turbulence versus instability effects, flame surface area increase downstream of obstacles, etc.) [87].

The present review highlights the value of coordinated efforts to develop improved consequence models. The parallel development tracks of several different CFD models for simulating gas explosions in the 1990s, which was integrated with experimental campaigns that explored the underlying phenomena, resulted in significant improvements in the modelling approaches that are still in use today. Establishing a community where developers of PDR models share their experiences, relevant literature, verification exercises and validation data, discuss issues, suggest new

numerical methods, etc. would presumably lead to further progress in gas explosion modelling also in the futfure.

Acknowledgements

H. Hisken and T. Skjold gratefully acknowledge the financial support of the Research Council of Norway and the partners of the LowEmission centre through the project Hy4GET (project no. 336442). Anand Zambare and Vagesh D. Narasimhamurthy acknowledge the financial grant from the Data Analytics, Risk and Technology (DART) laboratory, American Express India Private Limited.

References

1. Bjerketvedt, D., Bakke, J. R., van Wingerden, K.: Gas explosion handbook. Journal of Hazardous Materials, 52(1), 1-150 (1997).
2. European Union: Directive 1999/92/EC of the European Parliament and of the Council of 16 December 1999 on minimum requirements for improving the safety and health protection of workers potentially at risk from explosive atmospheres (15th individual Directive within the meaning of Article 16(1) of Directive 89/391/EEC). Official Journal of the European Union (1999).
3. Forskrift om håndtering av brannfarlig, reaksjonsfarlig og trykksatt stoff samt utstyr og anlegg som benyttes ved håndteringen (in Norwegian) (FOR-2009-06-08-602), https://lovdata.no/dokument/SF/forskrift/2009-06-08-602, last accessed on 26.02.2025.
4. TNO: Methods for the determination of possible damage to people and objects resulting from releases of hazardous materials (Green Book). CPR 16E, First edition (1992).
5. Vysus Group: Guidelines for quantitative risk analysis of facilities handling hazardous substances (revised edition). Report for: The Norwegian Directorate for Civil Protection (DSB). Report no: PRJ11100262033/R1 (2021).
6. NORSOK Z-013:2024, Risk and emergency preparedness assessment.
7. van Wingerden, K.: Advances in explosion modelling. FABIG Newsletter, 62:9–20 (2013).
8. van Wingerden, K.: Gas explosion modelling – Looking back. Presentation at the International Process Safety Week (IPSW), 2-6 December 2024.
9. Schelkin, K.I.: Influence of tube roughness on the formation and detonation propagation in gas. Zhurnal Eksperimentalnoi i Teoreticheskoi Fiziki, 10, 823–827 (1940).
10. Moen, I.O., Donato, M., Knystautas, R., Lee, J.H.: Flame acceleration due to turbulence produced by obstacles. Combustion and Flame, 39(1), 21–32 (1980).
11. Hjertager, B. H.: Influence of turbulence on gas explosions. Journal of Hazardous Materials, 9(3), 315 – 346 (1984).
12. SCI: Dispersion & explosion characteristics of large vapour clouds, Volume I and II. Technical Report ED024, Steel Construction Institute (2014).
13. Pedersen, H.H., Enstad, G.A., Skjold, T., Brewerton, R.W.: The effect of vegetation with various degrees of foliage on gas explosions in a 1.5 m channel. Proceedings Seventh International Seminar on Fire and Explosion Hazards (ISFEH), Providence, 5-10 May 2013, Research Publishing, Singapore: 646–655 (2013). ISBN: 978-981-07-5936-0.
14. Oran, E. S.: Understanding explosions – from catastrophic accidents to creation of the universe. Proceedings of the Combustion Institute, 35(1), 1 – 35 (2015).
15. Skjold, T., Pedersen, H. H., Narasimhamurthy, V. D., Lakshmipathy, S., Pesch, L., Atanga, G. F., Folusiak, M., Bernard, L., Siccama, D., Storvik, I. E.: Pragmatic modelling of industrial explosions in complex geometries: review of the state-of-the-art and prospects for

the future. In Borisov, A. A. and Frolov, S. M., editors, Zel'dovich Memorial: Accomplishments in the Combustion Science in the last decade, volume 1, pages 70–74. Torus Press (2014).
16. Narasimhamurthy, V. D., Hisken, H., Atanga, G., Skjold, T.: Porosity/distributed resistance modelling for industrial CFD applications. In Skallerud, B. and Andersson, H., editors, 8th National Conference on Computational Mechanics (MekIT'15) (2015).
17. Patankar, S. V., Spalding, D. B.: Heat Exchangers: Design and Theory Sourcebook, chapter "A calculation procedure for the transient and steady-state behavior of shell-and-tube heat exchangers", pages 155–176. McGraw-Hill (1974).
18. Sha, W. T., Yang, C. I., Kao, T. T., Cho, S. M.: Multidimensional numerical modeling of heat exchangers. Journal of Heat Transfer, 104(3), 417–425 (1982).
19. Hjertager, B. H.: Three-dimensional modeling of flow, heat transfer, and combustion. Handbook of heat and mass transfer, chapter 41, pages 1303–1350. Gulf Publishing, Houston (1986).
20. Hjertager, B. H., Solberg, T., Nymoen, K. O.: Computer modelling of gas explosion propagation in offshore modules. Journal of Loss Prevention in the Process Industries, 5(3), 165-174 (1992).
21. Arntzen, B. J.: Modelling of turbulence and combustion for simulation of gas explosions in complex geometries. PhD thesis, Department of Energy and Process Engineering, Norwegian University of Science and Technology, Norway (1998).
22. Puttock, J., Chakraborty, D., Farmayan, W.: Gas explosion modelling using PDRFoam. In Tenth International Symposium on Hazards, Prevention, and Mitigation of Industrial Explosions Bergen, Norway, 10-14 June 2014.
23. Ferreira, T. D., Santos, R. G., Vianna, S. S. V.: A coupled finite volume method and Gilbert–Johnson–Keerthi distance algorithm for computational fluid dynamics modelling. Computer Methods in Applied Mechanics and Engineering, 352, 417-436 (2019).
24. Gexcon AS: FLACS-CFD 24.2 User Manual. Confidential report (only accessible to users of FLACS-CFD). Date: January 15, 2025.
25. Magnussen, B., Hjertager, B.H.: On mathematical modeling of turbulent combustion with special emphasis on soot formation and combustion. Symp. Int. Combust. 16 (1), 719-729 (1977).
26. Eckhoff, R.K.; Gass- og oljetåke-eksplosjoner på oljeproduksjonsplattformer: et datagrunnlag. Confidential Report, Chr. Michelsens Institutt, Ref. CMI nr. 76153-1, 27. januar 1977 (in Norwegian).
27. Howell, S., Evanger, T., Magnussen, B., Shearer, F., Keating, M., Skjold, T., Siccama, D.: Analysis Origins - KFX and FLACS: Modelling Explosions and Combustion and the Impact of Piper Alpha. NAFEMS, blog post, July 2018. Available from: https://www.nafems.org/blog/posts/analysis-origins-kfx-and-flacs/, last accessed on 21 January 2025.
28. Launder, B. E., Spalding, D. B.: The numerical computation of turbulent flows. Computer Methods in Applied Mechanics and Engineering, 3(2), 269–289 (1974).
29. Poinsot, T., Veynante, D.: Theoretical and numerical combustion. 3rd edition (2011).
30. Bakke, J.R., Hjertager, B.H.: Quasi-laminar/turbulent combustion modelling, real cloud generation and boundary conditions in the FLAGS-ICE code, CMI No. 865402.2, Chr. Michelsen Institute (1986).
31. Bakke, J.R.: DSC. thesis, Numerical simulation of gas explosions in two-dimensional geometries, University of Bergen, Bergen (1986).
32. Johnson, D.M., Allason, D., Cronin, P.M.: Large scale experimental research of VCEs – A summary from one viewpoint. Journal of Loss Prevention in the Process Industries, 89, 105287 (2024).

33. Gardner, D.J., Hulme, G., Hughes, D.J.: A survey of current predictive methods for explosion hazard assessments in the UK offshore industry. IChemE Symposium series no. 134, Paper 7. Proceedings of Hazards 12, 19 - 21 April 1994.
34. Popat, N. R., Catlin, C. A., Arntzen, B. J., Lindstedt, R. P., Hjertager, B. H., Solberg, T., Saeter, O., Van den Berg, A. C.: Investigation to improve the accuracy of computational fluid dynamic based explosion models. Journal of Hazardous Materials, 45, 1–25 (1996).
35. Hjertager, B. H., Solberg, T.: A review of computional fluid dynamics (CFD) modeling of gas explosions. In: Zarko, V.E., Weiser, V., Eisenreich, N., Vasil'ev, A.A. (eds) Prevention of Hazardous Fires and Explosions. NATO Science Series, vol 26. Springer, Dordrecht (1999).
36. Lea, C. J., Ledin, H. S.: A review of the state-of-the-art in gas explosion modelling, Health and Safety Laboratory report no. HSL/2002/02 (2002).
37. Catlin, C. A., Fairweather, M., Ibrahim, S. S.: Predictions of turbulent, premixed flame propagation in explosion tubes. Combustion and Flame, 102(1-2), 115-128 (1995).
38. Fairweather, M., Hargrave, G.K., Ibrahim, S.S., Walker, D.G.: Studies of premixed flame propagation in explosion tubes. Combustion and Flame, 116(4), 504-518 (1999).
39. Fairweather, M., Ibrahim, S.S., Jaggers, H., Walker, D.G.: Turbulent premixed flame propagation in a cylindrical vessel. Symposium (International) on Combustion, 26(1), 365-371 (1996).
40. Hjertager, B. H.: Computer modelling of turbulent gas explosions in complex 2D and 3D geometries. Journal of Hazardous Materials, 34(2), 173-197 (1993).
41. Sæter, O.: Modelling and simulation of gas explosions in complex geometries. Doktor ingeniøravhandling 1998:116, NTNU Trondheim, Norges teknisk-naturvitenskapelige universitet and Høgskolen i Telemark (1998).
42. Mekonnen, A. T.: Modeling and numerical simulation of gas explosions for industrial safety analyses. Master's thesis, Norwegian University of Science and Technology (NTNU), Faculty of Engineering Department of Energy and Process Engineering. June 2019.
43. DNV: Ask the experts series: Vapour cloud explosion modelling. Learn how to use Phast and KFX-EXSIM for vapour cloud explosion modelling. Webinar video (2022). Available from https://www.dnv.com/software/campaigns-2022/plant-ask-the-experts-vapour-cloud-explosion-modelling-webinar-video/, last accessed on 21.02.2025.
44. DNV: Improved CFD modelling of hydrogen explosions with EXSIM. Webinar video (2023). Available from https://www.dnv.com/software/campaigns-2023/plant-improved-cfd-modelling-of-hydrogen-explosions-with-exsim-webinar-video/, last accessed on 21.02.2025.
45. Catlin, C. A., Lindstedt, R. P.: Premixed turbulent burning velocities derived from mixing controlled reaction models with cold front quenching. Combustion and Flame, 85(3-4), 427–439 (1991).
46. Hisken, H.: Investigation of instability and turbulence effects on gas explosions: experiments and modelling. PhD thesis, University of Bergen (2018).
47. Bray, K. N. C.: Studies of the turbulent burning velocity. Proceedings: Mathematical and Physical Sciences, 431(1882), 315–335 (1990).
48. Sha, W. T., Launder, B. E.: A model for turbulent momentum and heat transport in large rod bundles. Technical Report Report ANL-77-73, Illinois: Argonne National Laboratory (1979).
49. Middha, P.: Development, use, and validation of the CFD tool FLACS for hydrogen safety studies. PhD thesis, Department of Physics and Technology, University of Bergen, Norway (2010).
50. Middha, P., Hansen, O. R.: Predicting deflagration to detonation transition in hydrogen explosions. Process Safety Progress, 27(3), 192–204 (2008).

51. Klausen, M.-J.: Vented gas and dust explosions – external explosions. Master thesis, University of Bergen (2016).
52. van Wingerden, C. J. M., Zeeuwen, J. P.: On the role of acoustically driven flame instabilities in vented gas explosions and their elimination. Combustion and Flame, 51:109–111 (1983).
53. Cooper, M. G., Fairweather, M., Tite, J. P.: On the mechanisms of pressure generation in vented explosions. Combustion and Flame, 65(1):1–14 (1986).
54. Bauwens, C. R., Chaffee, J., Dorofeev, S. B.: Effect of ignition location, vent size, and obstacles on vented explosion overpressures in propane-air mixtures. Combustion Science and Technology, 182(11-12):1915–1932 (2010).
55. Johnson, D.M., Pekalski, A., Tam, V. H. Y., Burgan, B.A., Hoorelbeke, P., Savvides, C., Allason, D.: Interpretation of damage caused by a vapor cloud explosion. *Proc Safety Prog*. 2020; 39, e12106.
56. SCI: Buncefield explosion mechanism phase 1, volume 1 and 2. Technical report, Steel Construction Institute. Crown copyright (2009).
57. SCI: Dispersion & explosion characteristics of large vapour clouds, Volume I and II. Technical Report ED024, Steel Construction Institute (2014).
58. Skjold, T., Hisken, H., Atanga, G., Narasimhamurthy, V. D., Lakshmipathy, S., Storvik, I. E., Pesch, L.: Modelling Escalating Accident Scenarios and the Use of Risk-reducing technology for Explosion safety (MEASURE), final report. Confidential. Technical report, Gexcon AS, Bergen, Norway (2017).
59. Davis, S., Merilo, E., Engel, D., Ziemba, A., Pinto, M., van Wingerden, K.: Large scale detonation testing: New findings in the prediction of DDTs at large scales. Journal of Loss Prevention in the Process Industries, 48, 345-357 (2017).
60. Hisken, H., Mauri, L., Atanga, G., Lucas, M., van Wingerden, K., Skjold, T., Quillatre, P., Dutertre, A., Marteau, T., Pekalski, A., Jenney, L., Allason, D., Johnson, M., Leprette, E., Jamois, D., Hébrard, J., Proust, C.: Assessing the influence of real releases on explosions: selected results from large scale experiments. Journal of Loss Prevention in the Process Industries, 72, September 2021, 104561 (2021).
61. Both, A.-L.: Parameter optimisation for the improved modelling of industrial-scale gas explosions, PhD thesis, University of Bergen, Norway (2019).
62. Both, A.-L., Atanga, G., Hisken, H.: CFD modelling of gas explosions: optimising sub-grid model parameters. Journal of Loss Prevention in the Process Industries, 60, 159-173 (2019).
63. Lucas, M., Atanga, G., Hisken, H., Skjold, T.: Simulating vented hydrogen deflagrations: Improved modelling in the CFD tool FLACS-hydrogen. International Journal of Hydrogen Energy, 46 (23), 12464-12473 (2020).
64. Lucas, M., Hisken, H., Skjold, T., Arntzen, B. J., van Wingerden, K.: CFD modelling of hydrogen and hydrogen-methane explosions – Analysis of varying concentration and reduced oxygen atmospheres. Journal of Loss Prevention in the Process Industries, 83, 105012 (2023).
65. van den Berg, A.C., Mercx, W.P.M., Mouilleau, Y., Hayhurst, C.J.: AutoReaGas - A CFD-Tool for gas explosion hazard analysis. International Conference and Exhibition Offshore Structural Design. Hazards Safety and Engineering, November 1994, London, United Kingdom (1994).
66. Salzano, E., Marra, F.S., Russo, G., Lee, J.H.S.: Numerical simulation of turbulent gas flames in tubes. Journal of Hazardous Materials, 95(3), 233-247 (2002).
67. Weller, H. G., Tabor, G., Gosman, A. D., Fureby, C.: Application of a flame-wrinkling LES combustion model to a turbulent mixing layer. Symposium (International) on Combustion, 27(1), 899–907 (1998).
68. Puttock, J., Walter, F., Chakraborty, D., Raghunath, S., Sathiah, P.: Numerical simulations of gas explosion using Porosity Distributed Resistance approach Part −1: Validation against

small-scale experiments. Journal of Loss Prevention in the Process Industries, 75, 104659 (2022).
69. Puttock, J.S., Yardley, M.R., Cresswell, T.M.: Prediction of vapour cloud explosions using the SCOPE model. Journal of Loss Prevention in the Process Industries, 13(3–5), 419-431 (2000).
70. Bradley, D., Lawes, M., Liu, K., Mansour, M. S.: Measurements and correlations of turbulent burning velocities over wide ranges of fuels and elevated pressures. Proceedings of the Combustion Institute, 34(1), 1519 – 1526 (2013).
71. Dhiman, M., Meysiva, V., Sathiah, P., Narasimhamurthy, V. D.: Porosity/Distributed Resistance (PDR) modelling in the CFD solver PDRFoam. In Recent Advances in Applied Mechanics: Lecture Notes in Mechanical Engineering, pp. 503-519 (2022).
72. Dhiman, M., Zambare, A., Sathiah, P., Narasimhamurthy, V. D.: CFD simulations of vapour cloud explosions using PDRFoam. Journal of Loss Prevention in the Process Industries, 85, 105164 (2023).
73. Zambare, A., Narasimhamurthy, V.D., Skjold, T., Hisken, H.: Modelling of vented hydrogen deflagrations in an ISO container using PDRFoam. International Journal of Hydrogen Energy, 59, 251-262 (2024).
74. Vianna, S. S. V., Cant, R. S.: Modified porosity approach and laminar flamelet modelling for advanced simulation of accidental explosions. Journal of Loss Prevention in the Process Industries, 23(1), 3–14 (2010).
75. Ferreira, T.D., Vianna, S.S.V.: The Gilbert Johnson Keerthi distance algorithm coupled with Computational Fluid Dynamics applied to gas explosion simulation. Process Safety and Environmental Protection, 130, 209-220 (2019).
76. Ferreira, T.D., Vianna, S.S.V.: Collision of convex objects for calculation of porous mesh in gas explosion simulation. Journal of Loss Prevention in the Process Industries, 69, 104347 (2021).
77. Quaresma, T.L.S., Ferreira, T.D., Vianna, S.S.V.: A hybrid BML-fractal approach for the mean reaction rate modelling of accidental gas explosions in partially confined obstructed geometries. Process Safety and Environmental Protection, 152, 414-426 (2021).
78. Quaresma, T.L.S., Ferreira, T.D., Vianna, S.S.V.: Alternative approaches to the reaction rate modelling in gas explosion simulation using STOKES. Journal of Loss Prevention in the Process Industries, 74, 104646 (2022).
79. Skjold, T., Hisken, H., Lakshmipathy, S., Atanga, G., Bernard, L., van Wingerden, M., Olsen, K.L., Holme, M.N., Turøy, N.M., Mykleby, M., van Wingerden, K.: Vented hydrogen deflagrations in containers: Effect of congestion for homogeneous and inhomogeneous mixtures. International Journal of Hydrogen Energy, 44(17), pp.8819-8832 (2019).
80. Lakshmipathy, S., Skjold, T., Hisken, H., Atanga, G.: Consequence models for vented hydrogen deflagrations: CFD vs engineering models. International Journal of Hydrogen Energy, 44, 8699-8710 (2019).
81. Savitzky, A., Golay, M.: Smoothing and differentiation of data by simplified least squares procedures. Analytical Chemistry, 36(8), pp.1627-1639 (1964).
82. Kong, D.: An experimental study of certain aspects of initiation and turbulent propagation of gas explosions. PhD thesis, University of Bergen, Norway (1996).
83. Kong, D., Sand, I. Ø.: Experimental investigation of gas explosion driven transient flow in the near wake of bluff bodies - pipe arrays and complex obstacles. Technical Report CMR-96-F20003, Christian Michelsen Research, Bergen, Norway (1996).
84. Vik, K.-A.: Comparison of burning velocity differences in a numerical explosion simulator. Master's thesis, Department of Physics and Technology, University of Bergen, Norway (2014).
85. Skjold T., Hisken H., Derempouka E., Lucas M., Johnson, D.M.: Strength of Knowledge in Risk Assessments for Fuel-Air Explosions in Complex Geometries: Implications for

Hydrogen Systems. Proceedings Tenth International Seminar on Fire and Explosion Hazards (ISFEH), Oslo, 22-27 May 2022. ISBN: 978-82-7206-721-1.
86. Lee, H.C., Dai, P., Wan, M., Lipatnikov, A.N.: Differential diffusion effects and super-adiabatic local temperature in lean hydrogen-air turbulent flames, (2025), available from https://doi.org/10.48550/arXiv.2504.06168 [article submitted for publication].
87. Vermorel, O., Quillatre, P., Poinsot, T.: LES of explosions in venting chamber: A test case for premixed turbulent combustion models. Combustion and Flame, 183, 207-223 (2017).
88. DNV: CFD simulation software for dispersions and fires: KFX software, web page, available from https://www.dnv.com/software/services/plant/kfx-computational-fluid-dynamics-cfd-simulation-software-for-fires-and-dispersions/, last accessed on 15.05.2025.